Published in final edited form as:
Diabetes. 2005 January ; 54(1): 234–242.

Aldose Reductase Inhibition Counteracts Oxidative-Nitrosative Stress and Poly(ADP-Ribose) Polymerase Activation in Tissue Sites for Diabetes Complications

Irina G. Obrosova[1,2], **Pal Pacher**[3], **Csaba Szabó**[4], **Zsuzsanna Zsengeller**[4], **Hiroko Hirooka**[5], **Martin J. Stevens**[1], and **Mark A. Yorek**[6]

[1]Department of Internal Medicine, University of Michigan, Ann Arbor, Michigan [2]Pennington Biomedical Research Center, Louisiana State University System, Baton Rouge, Louisiana [3]Laboratory of Physiological Studies, National Institutes of Health/National Institute on Alcohol Abuse and Alcoholism, Bethesda, Maryland [4]Inotek Pharmaceuticals, Beverly, Massachusetts [5]Drug Development Research Laboratories, Sanwa Kagaku Kenkyusho, Mie, Japan [6]Veterans Affairs Medical Center and Department of Internal Medicine, University of Iowa, Iowa City, Iowa

Abstract

This study evaluated the effects of aldose reductase inhibition on diabetes-induced oxidative-nitrosative stress and poly(ADP-ribose) polymerase (PARP) activation. In animal experiments, control and streptozotocin-induced diabetic rats were treated with or without the aldose reductase inhibitor (ARI) fidarestat (16 mg · kg^{-1} · day^{-1}) for 6 weeks starting from induction of diabetes. Sorbitol pathway intermediate, but not glucose, accumulation in sciatic nerve and retina was completely prevented in diabetic rats treated with fidarestat. Sciatic motor nerve conduction velocity, hindlimb digital sensory nerve conduction velocity, and sciatic nerve concentrations of two major nonenzymatic antioxidants, glutathione and ascorbate, were reduced in diabetic versus control rats, and these changes were prevented in diabetic rats treated with fidarestat. Fidarestat prevented the diabetes-induced increase in nitrotyrosine (a marker of peroxynitrite-induced injury) and poly(ADP-ribose) immunoreactivities in sciatic nerve and retina. Fidarestat counteracted increased superoxide formation in aorta and epineurial vessels and in in vitro studies using hyperglycemia-exposed endothelial cells, and the DCF test/flow cytometry confirmed the endothelial origin of this phenomenon. Fidarestat did not cause direct inhibition of PARP activity in a cell-free system containing PARP and NAD^+ but did counteract high-glucose–induced PARP activation in Schwann cells. In conclusion, aldose reductase inhibition counteracts diabetes-induced nitrosative stress and PARP activation in sciatic nerve and retina. These findings reveal the new beneficial properties of fidarestat, thus further justifying the ongoing clinical trials of this specific, potent, and low-toxic ARI.

The Diabetes Control and Complications Trial (1) and the U.K. Prospective Diabetes Study (2) established the importance of hyperglycemia in the pathogenesis of chronic complications of diabetes. Hyperglycemia is involved in the pathogenesis of diabetic neuropathy, retinopathy, nephropathy, and macrovascular disease via multiple mechanisms, of which increased aldose reductase activity (3-5), nonenzymatic glycation and glycooxidation (6,7), activation of protein

Address correspondence and reprint requests to Irina G. Obrosova, PhD, Pennington Biomedical Research Center, Louisiana State University, 6400 Perkins Rd., Baton Rouge, LA 70808. obrosoig@pbrc.edu.
I.G.O. and P.P. contributed equally to this study.

kinase C (PKC) (8,9), and oxidative-nitrosative stress (10,11) are the best studied. More recently, it has been established that reactive oxygen and nitrogen species trigger activation of mitogen-activated protein kinases (MAPKs) and poly(ADP-ribose) polymerase (PARP), as well as the inflammatory cascade, and these downstream mechanisms are also involved in the pathogenesis of diabetes complications (12-15). The interactions among various hyperglycemia-initiated mechanisms are not completely understood, and the relationship between increased aldose reductase activity and oxidative-nitrosative stress/PARP activation has recently become a focus of interest. According to several studies performed in the diabetic lens (16,17), nerve (4,10,18), retina (19), and high-glucose–exposed endothelial cells (19,20), increased aldose reductase activity leads to oxidative stress. However, it has also been reported that increased aldose reductase activity is a consequence rather than a cause of oxidative stress (in particular, mitochondrial superoxide production) and PARP activation in the pathogenesis of diabetes complications (21).

Taking the above-mentioned details into account, the present study was designed to evaluate the effect of pharmacological aldose reductase inhibition with the potent and highly specific aldose reductase inhibitor (ARI) fidarestat (5,19,22-25) on diabetes-associated oxidative-nitrosative stress and PARP activation. Fidarestat has been extensively studied in experimental models of diabetic neuropathy and retinopathy and has been shown to prevent peripheral nerve dysfunction, signal transduction, and morphometric changes characteristic of diabetic neuropathy (22,23), as well as capillary cell loss (5), VEGF overexpression (19), increased vascular permealibility (24), and high-glucose–induced pericyte apoptosis (25) characteristic for diabetic retinopathy. Our animal studies performed in the streptozotocin (STZ)-induced diabetic rat model and in vitro studies in high-glucose–exposed endothelial and Schwann cells *1*) provide the first evidence of the key role for increased aldose reductase activity in nitrosative stress and PARP activation and *2*) support and complement previous observations of aldose reductase contribution to superoxide generation and antioxidant loss in tissue sites for diabetes complications.

RESEARCH DESIGN AND METHODS

The experiments were performed in accordance with regulations specified by the National Institutes of Health Principles of Laboratory Animal Care 1985 Revised Version and the University of Michigan and University of Iowa Protocols for Animal Studies.

Unless otherwise stated, all chemicals were of reagent-grade quality and purchased from Sigma Chemical (St. Louis, MO). Methanol (high-performance liquid chromatography grade), perchloric acid, hydrochloric acid, and sodium hydroxide were obtained from Fisher Scientific (Pittsburgh, PA). Reagents for immunohistochemistry have been purchased from Vector Laboratories (Burlingdale, CA) and Dako Laboratories (Santa Barbara, CA), as specified in the procedures. Bovine aortic endothelial cells (BAECs) and BAEC growth medium were purchased from Cambrex Bio Science Rockland (Rockland, ME) and rat Schwann cells (RCS96) from American *Type Culture* Collection (Manassas, VA).

Male Wistar rats (Charles River, Wilmington, MA) weighing 250–300 g were fed a standard rat diet (PMI Nutrition Int., Brentwood, MO) and had access to water ad libitum. Diabetes was induced with STZ as previously described (4,17,19). Blood samples for glucose measurements were taken from the tail vein ~48 h after the STZ injection and the day before the animals were killed. Rats with blood glucose ≥13.8 mmol/l were considered diabetic. The experimental groups comprised control and diabetic rats treated with or without fidarestat (16 mg · kg^{-1} · day^{-1}, in the diet). The treatments were started immediately after induction of diabetes. The duration of treatment was 6 weeks.

Anesthesia, euthanasia, and tissue sampling

Rats were anesthetized by inactin (65–85 mg/kg body wt i.p.). The onset (before induction of diabetes) motor nerve conduction velocity (MNCV) and sensory nerve conduction velocity (SNCV) measurements were followed by the final (6-week time point) measurements. In all measurements, body temperature was monitored by a rectal probe and maintained at 37°C with a warming pad. Hindlimb skin temperature was also monitored by a thermistor and maintained between 36 and 38°C by radiant heat. After completion of nerve functional measurements, the animals were sedated by CO_2 in a specially designed chamber (26) and immediately killed by cervical dislocation. The left nerve and retina were rapidly dissected, blotted with fine filter paper to remove any accompanying blood, and frozen in liquid nitrogen for subsequent measurements of glucose and sorbitol pathway intermediates. The nerve material was also used for assessment of glutathione (GSH) and ascorbate concentrations as well as fidarestat concentrations (fidarestat-treated control and diabetic groups). The right nerve and retina were fixed in formalin and later used for assessment of nitrotyrosine and poly(ADP-ribose) by immunohistochemistry. In some rats from the control, untreated diabetic, and fidarestat-treated diabetic groups (n = 4–5 per group), sciatic nerves were used for isolation of epineurial arterioles and subsequent assessment of arteriolar superoxide anion radical and nitrotyrosine abundance. Aortas from these rats were also sampled and immediately used for superoxide measurements.

Sciatic nerve epineurial arterioles were isolated as previously described (27)

BAECs were cultured in the BAEC growth medium containing 7 mmol/l glucose, according to the manufacturer's instructions. Rat Schwann cells 96 (RSC96) were cultured in Dulbecco's modified Eagle's medium (5.5 mmol/l glucose) containing 10% fetal bovine serum and a penicillin-streptomycin mixture (Invitrogen, Carlsbad, CA). The final concentrations in the culture medium are 100 μg/ml streptomycin and 100 units/ml penicillin. We used passages 5–12 for experiments with both cell types. Sciatic MNCV and hindlimb SNCV measurements were performed as described (4).

Glucose, sorbitol, and fructose concentrations in sciatic nerve and retina were assessed spectrofluorometrically by enzymatic procedures with hexokinase/glucose 6-phosphate dehydrogenase, sorbitol dehydrogenase, and fructose dehydrogenase as described (26). GSH and ascorbate concentrations in the sciatic nerve have been measured spectrofluorometrically with *O*-phthaldialdehyde and *O*-phenylenediamine, respectively (4).

All immunohistochemical samples were coded and examined by a single investigator in a blinded fashion. Microphotographs of stained sciatic nerves and retinas were taken with a Zeiss Axiolab microscope equipped with a Fuji HC-300C digital camera.

Nitrotyrosine immunoreactivity

Sciatic nerves and eyes were fixed in 4% paraformaldehyde in PBS, and 5-μm sections were prepared from paraffinembedded tissues. Endogenous peroxidase was quenched with 0.3% H_2O_2 in 60% methanol for 15 min. The sections were incubated overnight with 1:1,000–1:2,000 dilution of primary anti-nitrotyrosine antibody (Upstate Biotechnology, Lake Placid, NY). In control measurements, tissues were incubated with the primary antibody in the presence of 10 mmol/l nitrotyrosine. Specific labeling was detected with a biotin-conjugated goat anti-rabbit IgG and avidin-biotin peroxidase complex, both of which were supplied in the Vector Elite kit (Vector Laboratories). Color was developed using the Nidiaminobenzidine substrate kit (Vector Laboratories). Sections were counter-stained with hematoxylin-eosin, dehydrated, and mounted in Permount. The photomicrographs shown are representative

sections (n = 5–6) for each experimental group. A similar staining procedure has been used for epineurial vessel sections.

Poly(ADP-ribose) immunoreactivity

Paraffin sections (5 μm) were loaded onto polysine-coated slides (Fisher, Atlanta, GA), deparaffinized, and rehydrated. Optimal staining was achieved with an antigen retrieval method that was performed in 10 mmol/l citric acid for 15 min. Endogenous peroxidase was quenched with 0.3% H_2O_2 in 60% methanol for 15 min. Sections were blocked with 2% normal goat serum at room temperature for 1–2 h and incubated overnight with 1:250–1:500 dilution of primary anti-poly(ADP)-ribose antibody (generous gift from Tulip Biolabs). Specific labeling was detected with a biotin-conjugated goat anti-chicken IgG and avidin-biotin peroxidase complex (Vector Laboratories). The enzymatic reaction product was enhanced with nickel cobalt to give a black precipitate, and the sections were counterstained with hematoxylin-eosin, dehydrated, and mounted in Permount. Positive controls included formalin-fixed, paraffin-embedded tissues from lipolysaccharide-treated rats. Negative controls included elimination of the primary antibody.

Superoxide in epineurial vessels and aorta

Superoxide anion radical (O_2^-) abundance in epineurial vessels was assessed by the hydroethidine method, as we have described in detail (27). Vessels from control rats and untreated and treated diabetic rats were processed and imaged in parallel. Laser settings were identical for acquisition of all images from control and diabetic specimens.

Superoxide anion radical (O_2^-) abundance in aorta was measured by lucigenin-enhanced chemiluminescence, as previously described (27). Vessel segments were incubated in 0.5 ml PBS containing lucigenin (5 μmol/l); afterward, relative light units (RLUs) were measured using a Zylux FB12 luminometer. For these studies, chemiluminescence was measured for 5 min. Background activity was determined and subtracted, and RLUs were normalized to surface area.

Intracellular oxidative stress in BAECs

The BAECs were cultured (a six-well plate per condition) in the BAEC growth medium containing 7 mmol/l glucose, 30 mmol/l glucose, or 30 mmol/l glucose plus 1 μmol/l fidarestat (added for 4 h at the end of experiment). The total duration of the experiment was 4 days. Ten microliters of 10 μmol/l CM-H_2DCFDA, the dichlorofluorescein derivative with the best retention properties among all the studied analogs, was added for 30 min at the end of the experiment. The cells were then washed and trypsinized, and CM-H_2DCFDA fluorescence, an index of reactive oxygen species generation, was measured by flow cytometry (λ excitation, 480 nm; λ emission, 520 nm). After flow cytometry, the BAECs were counted and CM-H_2DCFDA fluorescence expressed per 10^6 cells.

Poly(ADP-ribose) in rat Schwann cells and cell-free system

For detection of poly(ADP-ribose) formed in Schwann cells, ~9,000 RSC96 in their growth media were seeded in each well of a 96-well enzyme-linked immunosorbent assay plate. After 24 h, the media were discarded and replaced by the new media containing 5.5 mmol/l glucose, 30 mmol/l glucose, or 30 mmol/l glucose plus 1 μmol/l fidarestat, for another 8 h, before CELISA (cell enzyme-linked immunosorbent assay) using the Poly(ADP-ribose) Polymerase Activity Assay Kit (Trevigen, Gaithersburg, MD). For detection of poly(ADP-ribose) formed in cell-free system, wells were coated with 1 mg/ml histone (50 μl/well) at 4°C overnight. Then, they were washed four times with PBS and blocked by adding 50 μl Strep-Diluent (supplied with the Trevigen kit). After incubation (1 h at room temperature), plates were washed

four times with PBS. Appropriate dilutions of fidarestat were combined with a 2× PARP cocktail (1.95 mmol/l NAD^+, 50 μmol/l biotinylated NAD^+ in 50 mmol/l Tris, pH 8.0, and 25 mmol/l $MgCl_2$) and high-specific activity PARP enzyme (both supplied with the Trevigen kit) in a 50-μl volume. The reaction was allowed to proceed for 30 min at room temperature before CELISA, which was performed according to the manufacturer's instructions. The results have been expressed as a percentage of the activity observed with no fidarestat present.

Fidarestat assessment in the sciatic nerve

The homogenate was prepared by disrupting frozen segments of rat sciatic nerve (~10–15 mg) in a mortar with distilled water. Internal standard solution of 8-fluoro-fidarestat was added to nerve homogenates. For calibration standards, a standard solution of fidarestat and internal standard was added to blank nerve homogenates. The homogenates were extracted four times with ethyl acetate, and the organic layers were evaporated to dryness. The residues were dissolved in the liquid chromatography–tandem mass spectrometry mobile phase, i.e., 0.2% AcOH/CH_3CN (7:3). The solutions were filtered and fidarestat concentrations quantified using a liquid chromatography–tandem mass spectrometer (TSQ7000; Thermo Electron, Finnigan, MA).

Statistical analysis

The results are expressed as means ± SE. Data were subjected to equality of variance *F* test and then to log transformation, if necessary, before one-way ANOVA. Where overall significance ($P < 0.05$) was attained, individual between-group comparisons were made using the Student-Newman-Keuls multiple-range test. Significance was defined at $P < 0.05$. When between-group variance differences could not be normalized by log transformation (datasets for body weights, plasma glucose, and some metabolic parameters), the data were analyzed by nonparametric Kruskal-Wallis one-way ANOVA followed by the Bonferroni/Dunn test for multiple comparisons.

RESULTS

The final body weights were comparably lower in untreated and fidarestat-treated diabetic rats than in the control group (Table 1). The final blood glucose concentrations were similarly elevated in untreated and fidarestat-treated diabetic rats compared with control rats.

Glucose, sorbitol, and fructose concentrations in sciatic nerve and retina were increased in diabetic rats compared with controls (Table 2). Fidarestat treatment did not affect glucose concentrations but essentially normalized sorbitol and fructose concentrations in sciatic nerve and retina of diabetic rats.

The onset MNCVs and SNCVs (both in m/s) were 54.7 ± 0.6 and 36.3 ± 0.3 in control rats, 55.1 ± 0.7 and 36.6 ± 0.4 in control rats treated with fidarestat, 54.6 ± 0.7 and 36.2 ± 0.4 in diabetic rats, and 54.3 ± 3 0.7 and 36.4 ± 0.5 in diabetic rats treated with fidarestat. The final MNCVs and SNCVs were reduced in diabetic rats compared with controls. Fidarestat treatment prevented both MNCV and SNCV slowing in diabetic rats without affecting either variable in control rats (Fig. 1). Sciatic nerve GSH and ascorbate concentrations were decreased in diabetic rats compared with controls (Fig. 2). Fidarestat treatment prevented nerve GSH and ascorbate depletion in diabetic rats without affecting those variables in control rats.

The sciatic nerve fidarestat concentration was 4.41 ± 0.23 nmol/g wet wt in fidarestat-treated control rats and 4.59 ± 0.29 nmol/g wet wt in fidarestat-treated diabetic rats.

Nitrotyrosine immunoreactivities were increased in sciatic nerve and retina of diabetic rats compared with controls, and this increase was markedly reduced by fidarestat treatment in both

tissues (Fig. 3*A*). In a similar fashion, the diabetes-associated increase in poly(ADP-ribose) immunoreactivity in sciatic nerve and retina was less manifest in diabetic rats treated with fidarestat than in untreated diabetic rats (Fig. 3*B*).

Superoxide and nitrotyrosine immunoreactivities were increased in epineurial vessels of diabetic rats compared with controls (Fig. 4*A* and *B*). The diabetes-associated increase in both immunoreactivities was markedly prevented by fidarestat treatment.

Superoxide abundance in aorta was significantly increased in diabetic compared with control rats (2.95 ± 0.21 and 1.64 ± 0.20 RLU, respectively, $P < 0.01$), and this increase was prevented by fidarestat treatment (1.52 ± 0.16 RLU, $P < 0.01$ vs. untreated diabetic group).

CM-H_2DCFDA fluorescence was increased in BAECs cultured in 30 mmol/l glucose compared with those cultured in 7 mmol/l glucose (Fig. 5*A*). This increase was completely corrected by fidarestat. Poly(ADP-ribose) abundance was increased in RSC96 cultured in 30 mmol/l glucose compared with those cultured in 5.5 mmol/l glucose (Fig. 5*B*), and this increase was prevented by fidarestat. Fidarestat, in the concentration range of 10 nmol/l to 100 μmol/l, did not affect PARP activity in the cell-free system containing PARP and NAD^+ (Table 3).

DISCUSSION

Numerous findings implicate increased aldose reductase activity in the pathogenesis of diabetic neuropathy (3-5,8,10,22), retinopathy (3,5,19,24,25,28), nephropathy (3), and macrovascular disease (3). The role for aldose reductase in the pathogenesis of diabetes complications is supported by, at least, four lines of evidence: *1*) similarity of physiological, metabolic, and morphological abnormalities in animal models of diabetes and galactose feeding (29,30); *2*) prevention, reversal, or slowing of diabetes complications by structurally diverse ARIs (3-5, 19,22,28,30); *3*) findings in cell culture models indicating that aldose reductase overexpression causes and aldose reductase inhibition corrects hyperglycemia-induced metabolic and gene expression abnormalities (31,32); and *4*) aldose reductase gene polymorphism data obtained in human subjects with diabetes (3). The role for aldose reductase in the pathogenesis of diabetic neuropathy is also supported by *1*) the presence of more severe diabetic and diabetes-like neuropathy in aldose reductase–overexpressing mice compared with the wild-type mice with normal aldose reductase content (33); *2*) clinical trials of the ARIs zenarestat (34) and fidarestat (35), indicating that robust aldose reductase inhibition in patients with diabetes improves peripheral nerve function and morphology; and *3*) identification of a high–aldose reductase protein level as an independent risk factor for diabetic neuropathy in patients with both type 1 and type 2 diabetes (3). The mechanism(s) of aldose reductase involvement in the pathogenesis of diabetes complications is not completely understood. Early studies revealed that increased aldose reductase activity leads to sorbitol accumulation and resulting osmotic stress (16,36). Later, increased aldose reductase activity has also been found to result in a variety of biochemical abnormalities, including *myo*-inositol depletion and downregulation of Na/KATP-ase activity (32,37), NAD^+/NADH and $NADP^+$/NADPH redox imbalances (4,17), changes in fatty acid metabolism (38), impaired neurotrophic support (39), and upregulation of vascular endothelial growth factor (19). Some of these disturbances (*myo*-inositol depletion) are obviously related to and some [$NAD(P)^+$/NAD(P)H redox changes] are independent of intracellular osmotic stress. Here, we demonstrate that increased aldose reductase activity is a major contributor to oxidative-nitrosative stress and PARP activation in diabetic peripheral nerve and retina.

Our animal studies have documented increased superoxide production in epineurial vessels of diabetic rats, and in vitro experiments with BAECs confirmed the endothelial origin of this phenomenon. Increased superoxide production in *vasa nervorum* correlated with that in large

vessels (aorta). Aldose reductase inhibition with fidarestat clearly prevented diabetes-associated superoxide formation in both aorta and epineurial vessels. These findings are consistent with several other reports indicating that structurally diverse ARIs, fidarestat (19) and zopolrestat (20,40), prevent hyperglycemia-induced superoxide formation (assessed by several different methods [19,20,40]) in aorta and retinal endothelial cells. We have also documented the presence of peroxynitrite-induced injury in peripheral nerve, epineurial vessels, and retina in diabetic rats. Peroxynitrite ($ONOO^-$) is a potent oxidant that causes *1*) initiation of lipid peroxidation; *2*) DNA breakage and base modification; *3*) protein (tyrosine amino acid) nitration and nitrosylation; *4*) alterations in cell signaling; and, *5*) in cases of severe damage, induction of cell necrosis and apoptosis (41). Nitrotyrosine immunoreactivities in sciatic nerve, epineurial vessels, and retina were reduced by fidarestat treatment. The latter is quite understandable, considering that peroxynitrite is a product of superoxide anion radical reaction with nitric oxide and that aldose reductase inhibition decreases superoxide abundance.

Growing evidence indicates that increased aldose reductase activity leads to diabetes-associated oxidative-nitrosative stress via several mechanisms. First, aldose reductase is responsible for downregulation of antioxidative defense provided by both nonenzymatic antioxidants, i.e., GSH, ascorbate (4,16,17 and current study), and taurine (31), and antioxidative defense enzymes, i.e., superoxide dismutase, catalase, glutathione peroxidase, glutathione reductase, and glutathione transferase (10,19). The mechanisms underlying this phenomenon are not clear. Both osmotic stress (10,16,26) and NADPH deficiency (33,42) have been implicated in diabetes-induced GSH depletion in lens and peripheral nerve. However, on the one hand, some findings in aldose reductase–transgenic mice are not consistent with the osmotic origin of oxidative stress (42). On the other hand, NADPH deficiency and related increase in oxidized glutathione (GSSG) concentration (a half-molar equivalent of GSH depletion) have never been experimentally documented in tissue sites for diabetes complications. In reality, GSSG concentrations in peripheral nerve, retina, and kidney are very low (<5% of GSH concentrations [10,17,19]) and diabetes-associated increase is either minimal or absent (10,17). Osmotic stress is clearly implicated in the depletion of another important nonenzymatic antioxidant, taurine (31).

In addition to disruption of antioxidative defense, increased aldose reductase activity contributes to oxidative-nitrosative stress indirectly via other pathways. Aldose reductase is involved in the generation of fructose, a glycation agent that is 10 times more potent than glucose. Increased aldose reductase activity results in formation of other precursors of advanced glycation end products (AGEs), i.e., methylglyoxal and 3-deoxyglucosone (43,44), and the AGEs pentosidine and carboxymethyllysine per se (45,46). Several reports indicate that aldose reductase inhibition counteracts formation of AGEs (45,46), which are known to generate oxidative stress via interaction with their receptors (47). Thus, increased aldose reductase activity contributes to oxidative stress by promoting nonenzymatic glycation. So far, several groups have reported that increased aldose reductase activity leads to activation of PKC in glomerular mesangial cells (48), vasculature (49), and smooth muscle cells (50). The latter probably occurs due to a aldose reductase–dependent decrease in free cytosolic NAD^+/NADH ratio and associated diversion of the glycolytic flux toward the increased formation of α-glycerophosphate and -diacylglycerol, an activator of PKC. PKC is essentially required for phosphorylation (activation) of NAD(P)H oxidase, the superoxide-generating enzyme (51), which is particularly important in the vasculature (8,9,51). Therefore, increased aldose reductase activity can contribute to increased superoxide generation via activation of PKC.

The present study also provides evidence that increased aldose reductase activity is responsible for PARP activation in the diabetic nerve and retina as well as in high-glucose–exposed Schwann cells. PARP activation, a recently discovered fundamental mechanism in the pathogenesis of diabetic endothelial (13) and myocardial (52) dysfunction, peripheral

neuropathy (14), and retinopathy (53), is completely or partially prevented in the two tissues of diabetic rats treated with the ARI fidarestat. Aldose reductase colocalizes with PARP in both tissue targets for diabetes complications. In the retina, aldose reductase and PARP are localized primarily in the neural retina (28,53) (Fig. 2*B*). In the sciatic nerve, aldose reductase is primarily localized in Schwann cells (33), and PARP, as we have recently demonstrated using the Schwann cell marker S-100 (14), is primarily localized in the Schwann cell nuclei. PARP is also known to be present in endothelial cells (13,54,55), including peripheral nerve endothelial cells (14), and evidence for endothelial localization of aldose reductase is emerging (28). However, the vasculature constitutes only ~1% of the total rat retina and <5% of the sciatic nerve. Therefore, it is reasonable to assume that *1*) the vast majority of poly(ADP-ribosyl)ated proteins is contained in the neural elements of both tissues and *2*) the effect of aldose reductase inhibition on poly(ADP-ribose) accumulation detected by immunohistochemistry is primarily localized in neuronal and glial retinal cells and in peripheral nerve Schwann cells.

It has been considered for many years that hydantoin ARIs may have weak antioxidant properties (56). Using bovine retinal endothelial cells, we previously found that fidarestat does not affect oxidative stress caused by factors other than hyperglycemia, i.e., three different pro-oxidants (19). The weak antioxidant capacity, if any, cannot explain the effects of fidarestat on diabetic neuropathy and retinopathy because conventional antioxidants, and even such potent compounds as DL-α-lipoic acid, require administration at much higher doses to produce effects on two complications' end points and oxidative stress in diabetic retina and peripheral nerve (57,58). Here, we show that fidarestat does not directly inhibit PARP in the cell-free system containing PARP and NAD^+. Note that we have tested the PARP-inhibiting capacity of fidarestat with very high concentrations of the compound, i.e., up to 100 μmol/l. This concentration exceeds the tissue (peripheral nerve) concentrations in diabetic rats by >20-fold and the concentration used for Schwann cells by 100-fold.

Growing evidence suggests that aldose reductase inhibition and PARP inhibition similarly affect the key biochemical abnormalities developing in diabetic and hyperglycemic conditions. Both aldose reductase inhibition and PARP inhibition normalize peripheral nerve mitochondrial and cytosolic NAD^+/NADH ratios and energy deficiency (4,59), as well as retinal VEGF overexpression in STZ-induced diabetic rats (19,53). As we have discussed above, aldose reductase inhibition is known to prevent diabetes-induced diversion of the glycolytic flux from glyceraldehyde 3-phosphate dehydrogenase toward the formation of α-glycerophosphate (10), the PKC activator diacylglycerol (48), and methylglyoxal (43). All these changes are prevented by structurally diverse ARIs (10,43,48). Increased formation of methylglyoxal and PKC activation has also been recently found to occur under conditions of high-glucose–induced PARP activation and to be preventable by PARP inhibition (55), further supporting the link between increased aldose reductase activity and PARP activation in the pathogenesis of diabetes complications. We have not found any suppression of sorbitol pathway hyperactivity in either diabetic retina (53) or peripheral nerve (59) by three structurally diverse PARP inhibitors, which is consistent with the downstream localization of the oxidative stress–triggered PARP activation consequent to increased aldose reductase activity, in the pathogenesis of diabetic neuropathy and retinopathy.

Our present findings are consistent with other studies demonstrating prevention of MAPK activation with aldose reductase inhibition by the ARIs AL-1576 (60) and fidarestat (23). Increased aldose reductase activity is the most likely to lead to MAPK activation via oxidative stress because it is well known that reactive oxygen and nitrogen species cause activation of all three major subfamilies of MAPKs (12). Both PARP activation and MAPK activation are involved in transcriptional regulation of gene expression via the transcription factors nuclear factor κB, activator protein-1, p53, and others (61,62). Activation of these transcription factors

leads to upregulation of inducible nitric oxide synthase, cyclooxygenase-2, endothelin-1, cell adhesion molecules, and inflammatory genes (61,63). Growing evidence indicates that all of these genes are involved in the pathogenesis of diabetes complications (15,64,65). The demonstration of a major contribution of aldose reductase to oxidative-nitrosative stress and PARP activation in tissue sites for diabetes complications allows us to predict that, in the near future, the link between increased aldose reductase activity and altered transcriptional regulation and gene expression will be established. It is important to realize that any product of genes controlled via PARP- and MAPK-dependent transcription factors, regardless of how unrelated it appears to be (from a biochemical viewpoint) to the sorbitol pathway, will be affected by a diabetes-associated increase in aldose reductase activity and amenable to control by aldose reductase inhibition.

In conclusion, our study generated evidence for the major role of increased aldose reductase activity in diabetes-associated oxidative-nitrosative stress and PARP activation. The data provide a rationale for studying the role for aldose reductase in diabetes-associated altered cell signaling, transcriptional regulation, and gene expression. The results reveal new beneficial properties of fidarestat, thus further justifying the ongoing clinical trials of this specific, potent, and low-toxic ARI.

Acknowledgments

The study was supported by an American Diabetes Association research grant (to I.G.O.), National Institutes of Health Grant DK59809-01 (to I.G.O.), Juvenile Diabetes Research Foundation Center for the Study of Complications of Diabetes Grant 4-200-421 (to I.G.O. and M.J.S.), National Institutes of Health Grant HL/DK 71215-01 (to C.S.), and National Institutes of Health Grant DK 058005-04 (to M.A.Y.).

The authors are grateful to Dr. Joseph Eichberg for valuable recommendations regarding the RSC96 cell culture experiments.

References

1. Writing Team for the Diabetes Control and Complications Trial/Epidemiology of Diabetes Interventions and Complications Research Group. Effect of intensive therapy on the microvascular complications of type 1 diabetes mellitus. JAMA 2002;287:2563–2569. [PubMed: 12020338]
2. UK Prospective Diabetes Study (UKPDS) Group. Intensive blood-glucose control with sulphonylureas or insulin compared with conventional treatment and risk of complications in patients with type 2 diabetes (UKPDS 33). Lancet 1998;352:837–853. [PubMed: 9742976]
3. Oates PJ, Mylari BL. Aldose reductase inhibitors: therapeutic implications for diabetic complications. Expert Opin Investig Drugs 1999;8:2095–2119.
4. Obrosova IG, Van Huysen C, Fathallah L, Cao XC, Greene DA, Stevens MJ. An aldose reductase inhibitor reverses early diabetes-induced changes in peripheral nerve function, metabolism, and antioxidative defense. FASEB J 2002;16:123–125. [PubMed: 11709499]
5. Kato N, Yashima S, Suzuki T, Nakayama Y, Jomori T. Long-term treatment with fidarestat suppresses the development of diabetic retinopathy in STZ-induced diabetic rats. J Diabetes Complications 2003;17:374–379. [PubMed: 14583184]
6. Thornalley PJ. Glycation in diabetic neuropathy: characteristics, consequences, causes, and therapeutic options. Int Rev Neurobiol 2002;50:37–57. [PubMed: 12198817]
7. Vlassara H, Palace MR. Glycoxidation: the menace of diabetes and aging. Mt Sinai J Med 2003;70:232–241. [PubMed: 12968196]
8. Nakamura J, Kato K, Hamada Y, Nakayama M, Chaya S, Nakashima E, Naruse K, Kasuya Y, Mizubayashi R, Miwa K, Yasuda Y, Kamiya H, Ienaga K, Sakakibara F, Koh N, Hotta N. A protein kinase C-β–selective inhibitor ameliorates neural dysfunction in streptozotocin-induced diabetic rats. Diabetes 1999;48:2090–2095. [PubMed: 10512378]
9. Way KJ, Katai N, King GL. Protein kinase C and the development of diabetic vascular complications. Diabet Med 2001;18:945–959. [PubMed: 11903393]

10. Obrosova IG. How does glucose generate oxidative stress in peripheral nerve? Int Rev Neurobiol 2002;50:3–35. [PubMed: 12198815]
11. Pennathur S, Heinecke JW. Mechanisms of oxidative stress in diabetes: implications for the pathogenesis of vascular disease and antioxidant therapy. Front Biosci 2004;9:565–574. [PubMed: 14766391]
12. Purves T, Middlemas A, Agthong S, Jude EB, Boulton AJ, Fernyhough P, Tomlinson DR. A role for mitogen-activated protein kinases in the etiology of diabetic neuropathy. FASEB J 2001;15:2508–2514. [PubMed: 11689477]
13. Garcia Soriano F, Virag L, Jagtap P, Szabo E, Mabley JG, Liaudet L, Marton A, Hoyt DG, Murthy KG, Salzman AL, Southan GJ, Szabo C. Diabetic endothelial dysfunction: the role of poly(ADP-ribose) polymerase activation. Nat Med 2001;7:108–113. [PubMed: 11135624]
14. Obrosova IG, Li F, Abatan OI, Forsell MA, Komjati K, Pacher P, Szabo C, Stevens MJ. Role of poly (ADP-ribose) polymerase activation in diabetic neuropathy. Diabetes 2004;53:711–720. [PubMed: 14988256]
15. Joussen AM, Poulaki V, Le ML, Koizumi K, Esser C, Janicki H, Schraermeyer U, Kociok N, Fauser S, Kirchhof B, Kern TS, Adamis AP. A central role for inflammation in the pathogenesis of diabetic retinopathy. FASEB J 2004;18:1450–1452. [PubMed: 15231732]
16. Lou MF, Dickerson JE Jr, Garadi R, York BM Jr. Glutathione depletion in the lens of galactosemic and diabetic rats. Exp Eye Res 1988;46:517–530. [PubMed: 3133235]
17. Obrosova IG, Fathallah L. Evaluation of an aldose reductase inhibitor on lens metabolism, ATPases and antioxidative defense in streptozotocin-diabetic rats: an intervention study. Diabetologia 2000;43:1048–1055. [PubMed: 10990083]
18. Lowitt S, Malone JI, Salem AF, Korthals J, Benford S. Acetyl-L-carnitine corrects the altered peripheral nerve function of experimental diabetes. Metabolism 1995;44:677–680. [PubMed: 7752919]
19. Obrosova IG, Minchenko AG, Vasupuram R, White L, Abatan OI, Kumagai AK, Frank RN, Stevens MJ. Aldose reductase inhibitor fidarestat prevents retinal oxidative stress and vascular endothelial growth factor overexpression in streptozotocin-diabetic rats. Diabetes 2003;52:864–871. [PubMed: 12606532]
20. El-Remessy AB, Abou-Mohamed G, Caldwell RW, Caldwell RB. High glucose-induced tyrosine nitration in endothelial cells: role of eNOS uncoupling and aldose reductase activation. Invest Ophthalmol Vis Sci 2003;44:3135–3143. [PubMed: 12824263]
21. Brownlee M. Biochemistry and molecular cell biology of diabetic complications. Nature 2001;414:813–820. [PubMed: 11742414]
22. Kato N, Mizuno K, Makino M, Suzuki T, Yagihashi S. Effects of 15-month aldose reductase inhibition with fidarestat on the experimental diabetic neuropathy in rats. Diabetes Res Clin Pract 2000;50:77–85. [PubMed: 10960717]
23. Price SA, Agthong S, Middlemas AB, Tomlinson DR. Mitogen-activated protein kinase p38 mediates reduced nerve conduction velocity in experimental diabetic neuropathy: interactions with aldose reductase. Diabetes 2004;53:1851–1856. [PubMed: 15220210]
24. Amano S, Yamagishi S, Kato N, Inagaki Y, Okamoto T, Makino M, Taniko K, Hirooka H, Jomori T, Takeuchi M. Sorbitol dehydrogenase overexpression potentiates glucose toxicity to cultured retinal pericytes. Biochem Biophys Res Commun 2002;299:183–188. [PubMed: 12437967]
25. Miwa K, Nakamura J, Hamada Y, Naruse K, Nakashima E, Kato K, Kasuya Y, Yasuda Y, Kamiya H, Hotta N. The role of polyol pathway in glucose-induced apoptosis of cultured retinal pericytes. Diabetes Res Clin Pract 2003;60:1–9. [PubMed: 12639759]
26. Obrosova IG, Fathallah L, Lang HJ, Greene DA. Evaluation of a sorbitol dehydrogenase inhibitor on diabetic peripheral nerve metabolism: a prevention study. Diabetologia 1999;42:1187–1194. [PubMed: 10525658]
27. Coppey LJ, Gellett JS, Davidson EP, Dunlap JA, Lund DD, Yorek MA. Effect of antioxidant treatment of streptozotocin-induced diabetic rats on endoneurial blood flow, motor nerve conduction velocity, and vascular reactivity of epineurial arterioles of the sciatic nerve. Diabetes 2001;50:1927–1937. [PubMed: 11473057]

28. Dagher Z, Park YS, Asnaghi V, Hoehn T, Gerhardinger C, Lorenzi M. Studies of rat and human retinas predict a role for the polyol pathway in human diabetic neuropathy. Diabetes 2004;53:2404–2411. [PubMed: 15331552]
29. Kern TS, Engerman RL. Comparison of retinal lesions in alloxan-diabetic rats and galactose-fed rats. Curr Eye Res 1994;13:863–867. [PubMed: 7720392]
30. Kador PF, Takahashi Y, Wyman M, Ferris F 3rd. Diabetes like proliferative retinal changes in galactose-fed dogs. Arch Ophthalmol 1995;113:352–354. [PubMed: 7887849]
31. Thomas TP, Porcellati F, Kato K, Stevens MJ, Sherman WR, Greene DA. Effects of glucose on sorbitol pathway activation, cellular redox, and metabolism of myo-inositol, phosphoinositide, and diacylglycerol in cultured human retinal pigment epithelial cells. J Clin Invest 1994;93:2718–2724. [PubMed: 8201009]
32. Stevens MJ, Hosaka Y, Masterson JA, Jones SM, Thomas TP, Larkin DD. Down-regulation of the human taurine transporter by glucose in cultured retinal pigment epithelial cells. Am J Physiol 1999;277:E760–E771. [PubMed: 10516137]
33. Song Z, Fu DT, Chan YS, Leung S, Chung SS, Chung SK. Transgenic mice overexpressing aldose reductase in Schwann cells show more severe nerve conduction velocity deficit and oxidative stress under hyperglycemic stress. Mol Cell Neurosci 2003;23:638–647. [PubMed: 12932443]
34. Greene DA, Arezzo JC, Brown MB. Effect of aldose reductase inhibition on nerve conduction and morphometry in diabetic neuropathy: Zenarestat Study Group. Neurology 1999;53:580–591. [PubMed: 10449124]
35. Hotta N, Toyota T, Matsuoka K, Shigeta Y, Kikkawa R, Kaneko T, Takahashi A, Sugimura K, Koike Y, Ishii J, Sakamoto N. SNK-860 Diabetic Neuropathy Study Group. Clinical efficacy of fidarestat, a novel aldose reductase inhibitor, for diabetic peripheral neuropathy: a 52-week multicenter placebo-controlled double-blind parallel group study. Diabetes Care 2001;24:1776–1782. [PubMed: 11574441]
36. Kador PF. The contributions of Jin H. Kinoshita to aldose reductase research. Exp Eye Res 1990;50:615–620. [PubMed: 2115449]
37. Sima AA, Dunlap JA, Davidson EP, Wiese TJ, Lightle RL, Greene DA, Yorek MA. Supplemental *myo*-inositol prevents l-fucose-induced diabetic neuropathy. Diabetes 1997;46:301–306. [PubMed: 9000708]
38. Kuruvilla R, Eichberg J. Depletion of phospholipid arachidonoyl-containing molecular species in a human Schwann cell line grown in elevated glucose and their restoration by an aldose reductase inhibitor. J Neurochem 1998;71:775–783. [PubMed: 9681469]
39. Ohi T, Saita K, Furukawa S, Ohta M, Hayashi K, Matsukura S. Therapeutic effects of aldose reductase inhibitor on experimental diabetic neuropathy through synthesis/secretion of nerve growth factor. Exp Neurol 1998;151:215–220. [PubMed: 9628756]
40. Gupta S, Chough E, Daley J, Oates P, Tornheim K, Ruderman NB, Keaney JF Jr. Hyperglycemia increases endothelial superoxide that impairs smooth muscle cell Na+-K+-ATPase activity. Am J Physiol Cell Physiol 2002;282:C560–C566. [PubMed: 11832341]
41. Virag L, Szabo E, Gergely P, Szabo C. Peroxynitrite-induced cytotoxicity: mechanism and opportunities for intervention (Review). Toxicol Lett 2003;140–141:113–124.
42. Lee AY, Chung SS. Contributions of polyol pathway to oxidative stress in diabetic cataract. FASEB J 1999;13:23–30. [PubMed: 9872926]
43. Phillips SA, Mirrlees D, Thornalley PJ. Modification of the glyoxalase system in streptozotocin-induced diabetic rats: effect of the aldose reductase inhibitor Statil. Biochem Pharmacol 1993;46:805–811. [PubMed: 8373434]
44. Beisswenger PJ, Howell SK, Nelson RG, Mauer M, Szwergold BS. Alpha-oxoaldehyde metabolism and diabetic complications. Biochem Soc Trans 2003;31:1358–1363. [PubMed: 14641063]
45. Nagaraj RH, Prabhakaram M, Ortwerth BJ, Monnier VM. Suppression of pentosidine formation in galactosemic rat lens by an inhibitor of aldose reductase. Diabetes 1994;43:580–586. [PubMed: 8138064]
46. Hamada Y, Nakamura J, Naruse K, Komori T, Kato K, Kasuya Y, Nagai R, Horiuchi S, Hotta N. Epalrestat, an aldose reductase ihibitor, reduces the levels of Nε-(carboxymethyl)lysine protein

adducts and their precursors in erythrocytes from diabetic patients. Diabetes Care 2000;23:1539–1544. [PubMed: 11023149]

47. Yan SF, Ramasamy R, Naka Y, Schmidt AM. Glycation, inflammation, and RAGE: a scaffold for the macrovascular complications of diabetes and beyond. Circ Res 2003;93:1159–1169. [PubMed: 14670831]
48. Keogh RJ, Dunlop ME, Larkins RG. Effect of inhibition of aldose reductase on glucose flux, diacylglycerol formation, protein kinase C, and phospholipase A2 activation. Metabolism 1997;46:41–47. [PubMed: 9005967]
49. Yamagishi S, Uehara K, Otsuki S, Yagihashi S. Differential influence of increased polyol pathway on protein kinase C expressions between endoneurial and epineurial tissues in diabetic mice. J Neurochem 2003;87:497–507. [PubMed: 14511127]
50. Nakamura J, Kasuya Y, Hamada Y, Nakashima E, Naruse K, Yasuda Y, Kato K, Hotta N. Glucose-induced hyperproliferation of cultured rat aortic smooth muscle cells through polyol pathway hyperactivity. Diabetologia 2001;44:480–487. [PubMed: 11357479]
51. Inoguchi T, Sonta T, Tsubouchi H, Etoh T, Kakimoto M, Sonoda N, Sato N, Sekiguchi N, Kobayashi K, Sumimoto H, Utsumi H, Nawata H. Protein kinase C-dependent increase in reactive oxygen species (ROS) production in vascular tissues of diabetes: role of vascular NAD(P)H oxidase. J Am Soc Nephrol 2003;14(Suppl 3):S227–S232. [PubMed: 12874436]
52. Pacher P, Liaudet L, Soriano FG, Mabley JG, Szabo E, Szabo C. The role of poly(ADP-ribose) polymerase activation in the development of myocardial and endothelial dysfunction in diabetes. Diabetes 2002;51:514–521. [PubMed: 11812763]
53. Obrosova IG, Minchenko AG, Frank RN, Seigel GM, Zsengeller Z, Pacher P, Stevens MJ, Szabo C. Poly(ADP-ribose) polymerase inhibitors counteract diabetes- and hypoxia-induced retinal vascular endothelial growth factor overexpression. Int J Mol Med 2004;14:55–64. [PubMed: 15202016]
54. Szabo C, Zanchi A, Komjati K, Pacher P, Krolewski AS, Quist WC, LoGerfo FW, Horton ES, Veves A. Poly(ADP-Ribose) polymerase is activated in subjects at risk of developing type 2 diabetes and is associated with impaired vascular reactivity. Circulation 2002;106:2680–2686. [PubMed: 12438293]
55. Du X, Matsumura T, Edelstein D, Rossetti L, Zsengeller Z, Szabo C, Brownlee M. Inhibition of GAPDH activity by poly(ADP-ribose) polymerase activates three major pathways of hyperglycemic damage in endothelial cells. J Clin Invest 2003;112:1049–1057. [PubMed: 14523042]
56. Ou P, Nourooz-Zadeh J, Tritschler HJ, Wolff S. Activation of aldose reductase in rat lens and metal-ion chelation by aldose reductase inhibitors and lipoic acid. Free Radic Res 1996;25:337–346. [PubMed: 8889497]
57. Stevens MJ, Obrosova I, Cao X, Van Huysen C, Greene DA. Effects of DL-α-lipoic acid on peripheral nerve conduction, blood flow, energy metabolism, and oxidative stress in experimental diabetic neuropathy. Diabetes 2000;49:1006–1015. [PubMed: 10866054]
58. Obrosova IG, Minchenko AG, Marinescu V, Fathallah L, Kennedy A, Stockert CM, Frank RN, Stevens MJ. Antioxidants attenuate early up regulation of retinal vascular endothelial growth factor in streptozotocin-diabetic rats. Diabetologia 2001;44:1102–1010. [PubMed: 11596663]
59. Li F, Szabo C, Pacher P, Southan GJ, Abatan OI, Charniauskaya T, Stevens MJ, Obrosova IG. Evaluation of orally active poly(ADP-ribose) polymerase inhibitor in streptozotocin-diabetic rat model of early peripheral neuropathy. Diabetologia 2004;47:710–717. [PubMed: 15298348]
60. Zatechka DS Jr, Kador PF, Garcia-Castineiras S, Lou MF. Diabetes can alter the signal transduction pathways in the lens of rats. Diabetes 52:1014–1022. [PubMed: 12663474]
61. Ha HC, Hester LD, Snyder SH. Poly(ADP-ribose) polymerase-1 dependence of stress-induced transcription factors and associated gene expression in glia. Proc Natl Acad Sci U S A 2002;99:3270–3275. [PubMed: 11854472]
62. Yang SH, Sharrocks AD, Whitmarsh AJ. Transcriptional regulation by the MAP kinase signaling cascades. Gene 2003;320:3–21. [PubMed: 14597384]
63. Minchenko AG, Stevens MJ, White L, Abatan OI, Komjati K, Pacher P, Szabo C, Obrosova IG. Diabetes-induced overexpression of endothelin-1 and endothelin receptors in the rat renal cortex is mediated via poly(ADP-ribose) polymerase activation. FASEB J 2003;17:1514–1516. [PubMed: 12824290]

64. Pop-Busui R, Marinescu V, Van Huysen C, Li F, Sullivan K, Greene DA, Larkin D, Stevens MJ. Dissection of metabolic, vascular, and nerve conduction interrelationships in experimental diabetic neuropathy by cyclooxygenase inhibition and acetyl-l-carnitine administration. Diabetes 2002;51:2619–2628. [PubMed: 12145179]

65. Baumgartner-Parzer SM. Glycemia and regulation of endothelial adhesion molecules. Horm Metab Res 1997;29:636–638. [PubMed: 9497902]

Glossary

AGE
advanced glycation end product

ARI
aldose reductase inhibitor

BAEC
bovine aortic endothelial cell

GSH
glutathione

MAPK
mitogen-activated protein kinase

MNCV
motor nerve conduction velocity

PARP
poly(ADP-ribose) polymerase

PKC
protein kinase C

RSC96
rat Schwann cells 96

SNCV
sensory nerve conduction velocity

STZ
streptozotocin

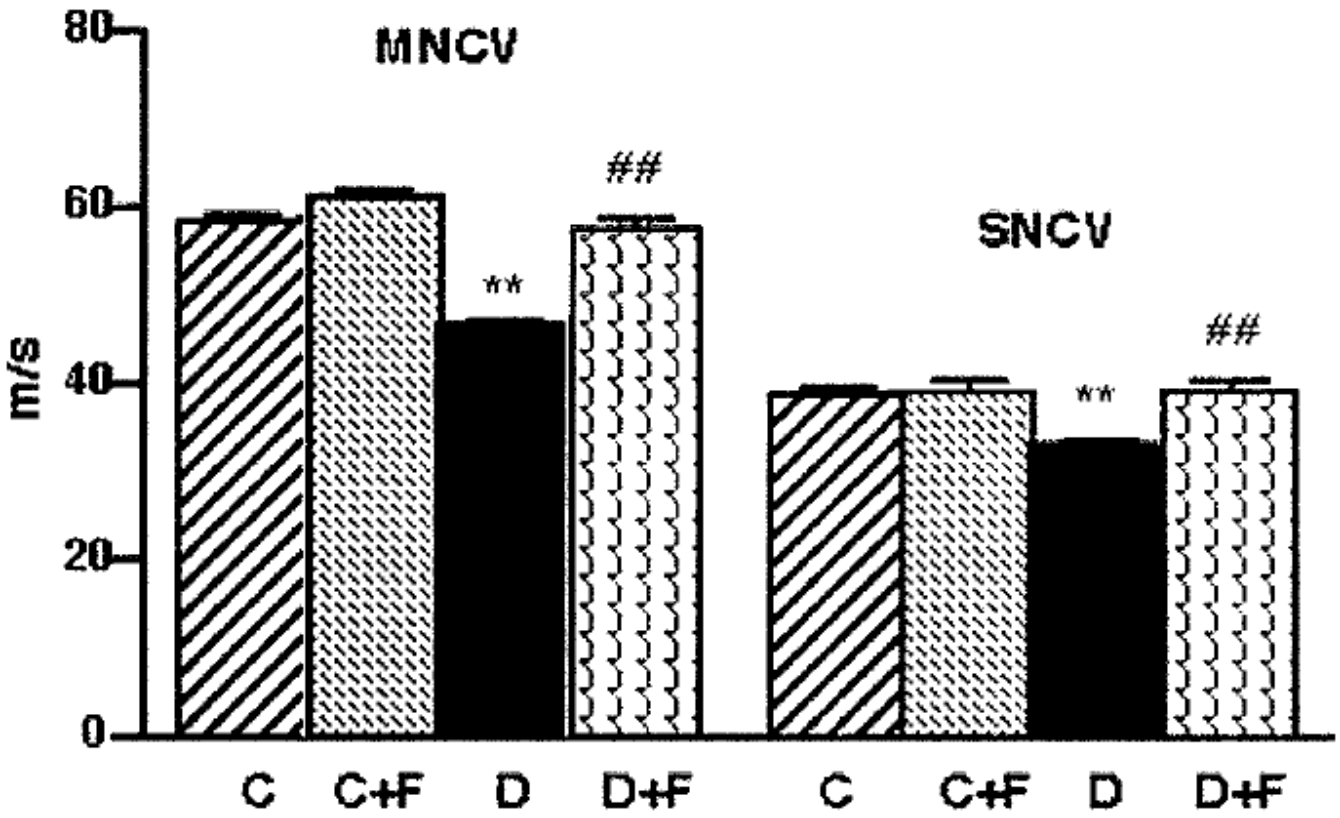

FIG. 1.

Final sciatic MNCVs and hindlimb digital SNCVs in control and STZ-induced diabetic rats treated with or without fidarestat. Results are means ± SE (n = 8–10 per group). C, control; D, diabetic; F, fidarestat. **P < 0.01 vs. control group; ##P < 0.01 vs. untreated diabetic group.

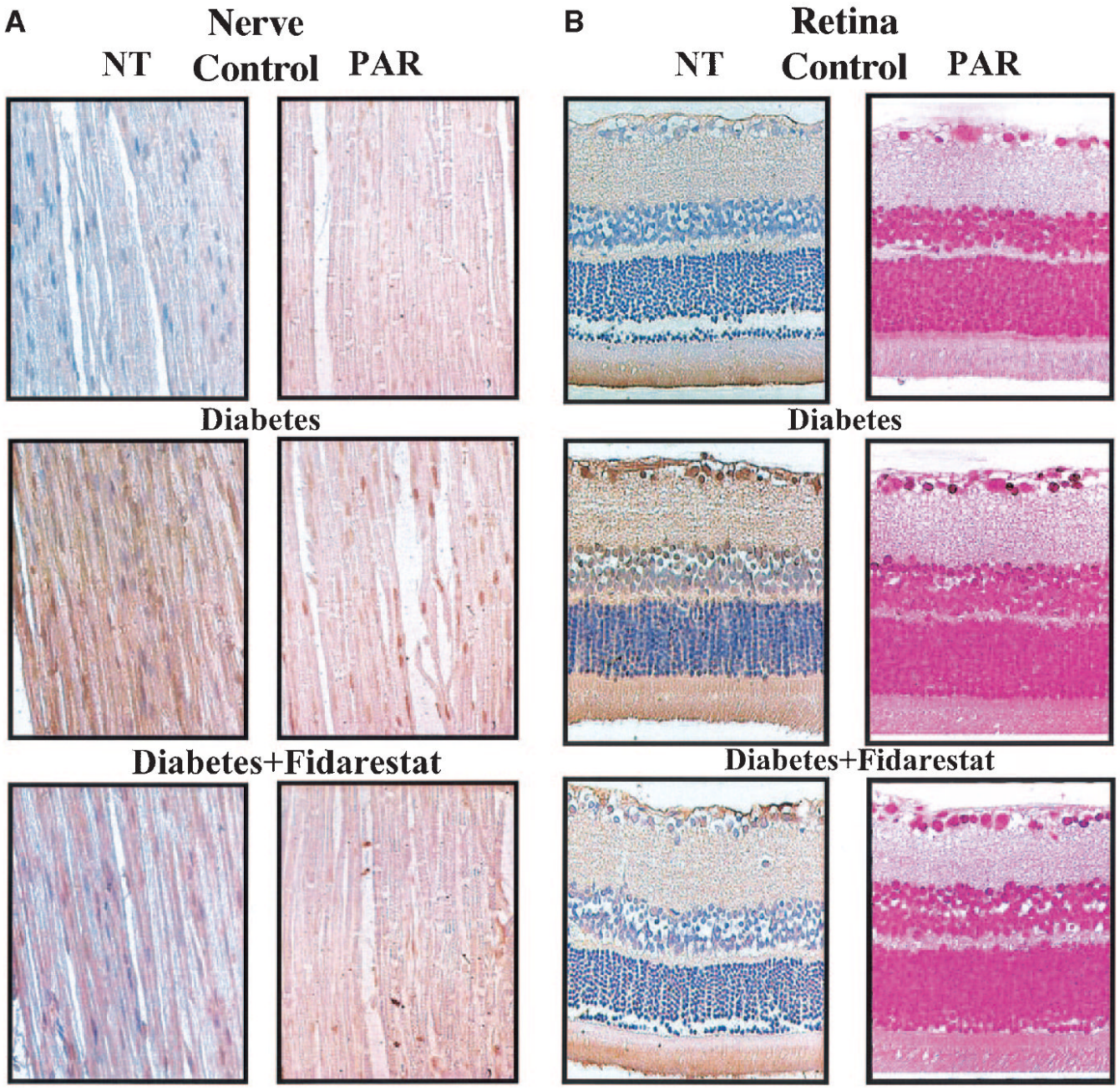

FIG. 2.

Representative microphotographs of immunohistochemical staining of nitrotyrosine and poly (ADP-ribose) in the sciatic nerve (*A*) and retina (*B*) in control rats, diabetic rats, and diabetic rats treated with fidarestat (n = 5–6 per group). Magnification ×400.

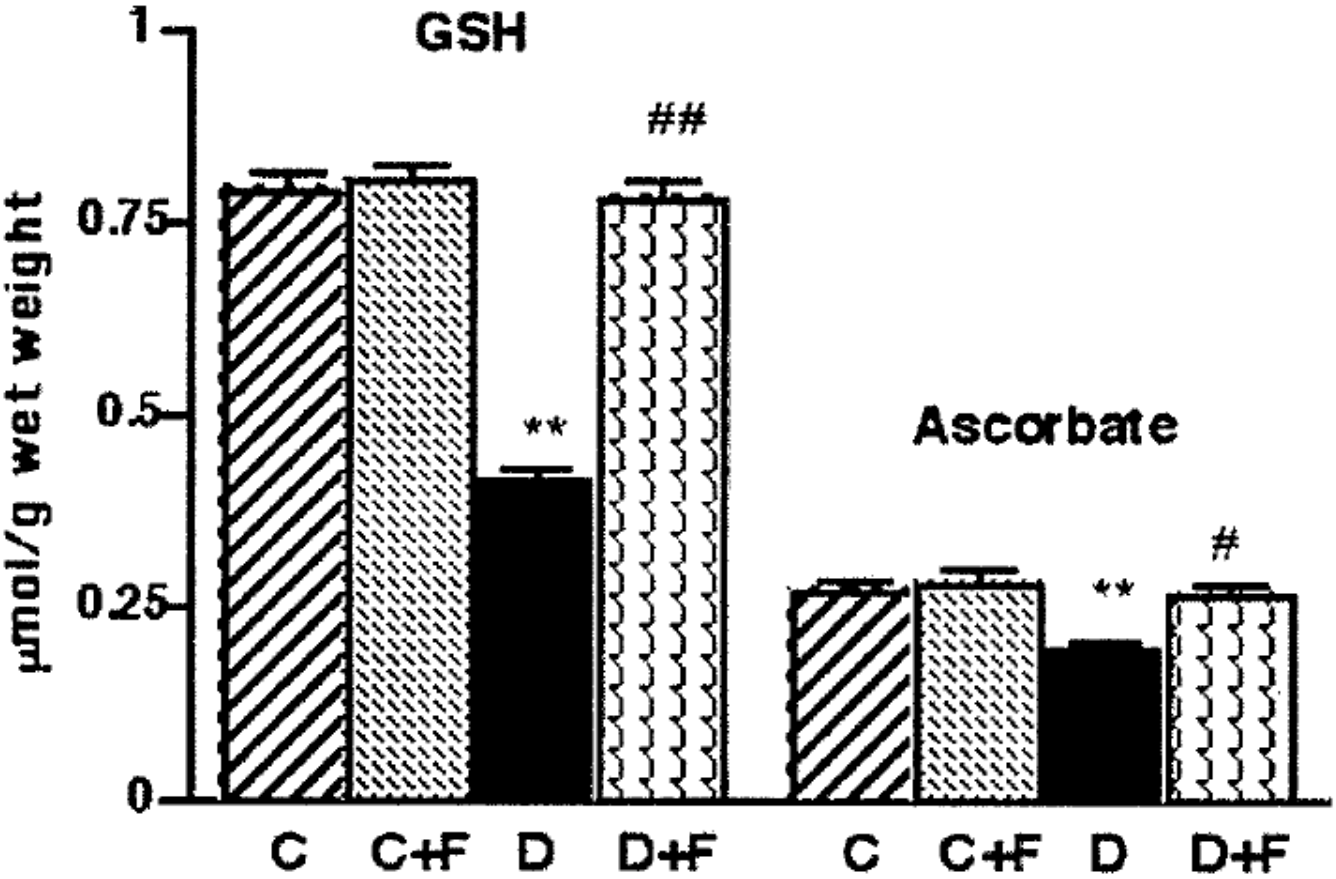

FIG. 3.

Sciatic nerve GSH and ascorbate concentrations in control and diabetic rats with and without fidarestat treatment. Results are means ± SE (n = 8 per group). C, control, D, diabetic; F, fidarestat. $^{**}P < 0.01$ vs control group; $^{\#}P < 0.05$, $^{\#\#}P < 0.01$ vs. untreated diabetic group.

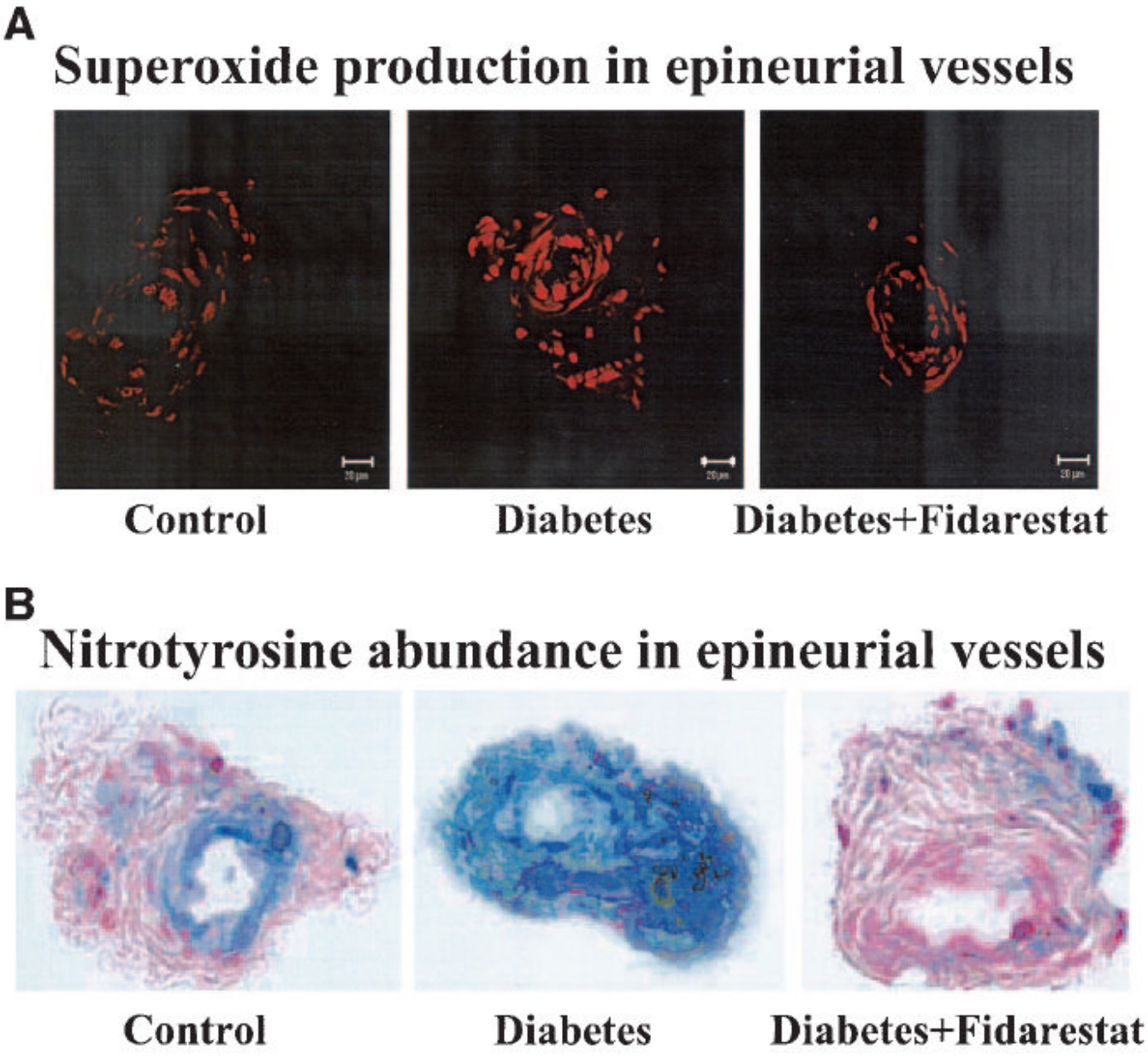

FIG. 4.

Representative microphotographs of superoxide-generated fluorescence and immunohistochemical staining of nitrotyrosine in sciatic nerve epineurial vessels in control rats, diabetic rats, and diabetic rats treated with fidarestat (n = 5–6 per group). Magnification ×40.

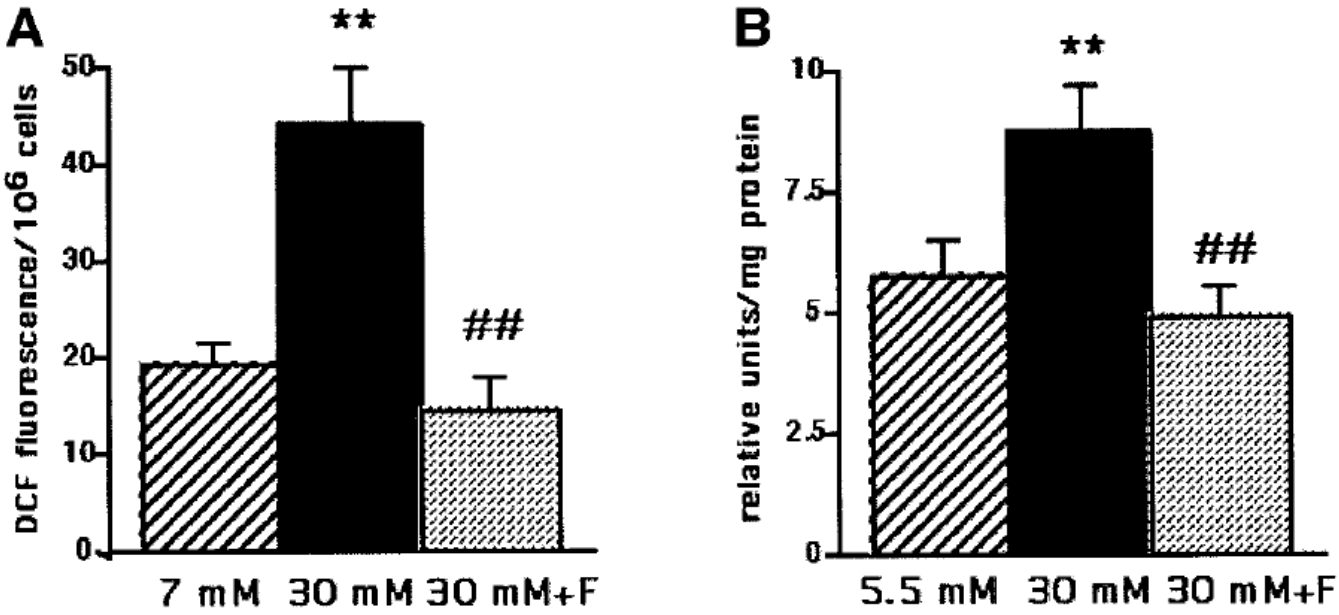

FIG. 5.

A: Intracellular reactive oxygen species abundance in BAECs cultured in 7 mmol/l glucose and 30 mmol/l glucose with and without 1 μmol/l fidarestat Results are means ± SE (n = 8–10 per group). **P < 0.01 vs. BAECs cultured in 7 mmol/l glucose; ##P < 0.01 vs. BAECs cultured in 30 mmol/l glucose without fidarestat. *B*: Poly-(ADP-ribose) activity [relative units of poly (ADP-ribose) per milligram protein] in RSC96 cultured in 5.5 mmol/l glucose, 30 mmol/l glucose, or 30 mmol/l glucose with 1 μmol/l fidarestat. Results are means ± SE (n = 8–10 per group). **P < 0.01 vs. RSC96 cultured in 5.5 mmol/l glucose; ##P < 0.01 vs. RSC96 cultured in 30 mmol/l glucose without fidarestat.

TABLE 1

Body weights and blood glucose concentrations in control and diabetic rats with and without fidarestat treatment

	Body weight (g)		Blood glucose
	Initial*	Final	(mmol/l)
Control	285 ± 7	483 ± 10	5.08 ± 0.21
Control plus fidarestat	292 ± 6	467 ± 9	5.24 ± 0.22
Diabetic	288 ± 7	350 ± 7†	18.8 ± 0.56†
Diabetic plus fidarestat	293 ± 6	342 ± 12†	19.4 ± 0.62†

Data are means ± SE (n = 20–25).

*Before induction of STZ diabetes.

†Significantly different from controls ($P < 0.01$).

TABLE 2

Sorbitol pathway intermediate concentrations* in sciatic nerve and retina of control and diabetic rats with and without fidarestat treatment

	Glucose	Sorbitol	Fructose
Sciatic nerve			
Control	3.39 ± 0.10	0.123 ± 0.010	1.20 ± 0.11
Control plus fidarestat	3.34 ± 0.12	0.129 ± 0.009	1.31 ± 0.07
Diabetic	13.9 ± 0.59†	1.30 ± 0.10†	5.57 ± 0.20†
Diabetic plus fidarestat	13.2 ± 0.54†	0.077 ± 0.007‡‡	1.30 ± 0.09‡‡
Retina			
Control	9.3 ± 0.73	1.75 ± 0.13	1.34 ± 0.25
Control plus fidarestat	10.2 ± 0.77	1.57 ± 0.14	1.28 ± 0.31
Diabetic	95 ± 7.4†	11.4 ± 0.81†	5.34 ± 0.52†
Diabetic plus fidarestat	106 ± 8.7†	1.81 ± 0.34‡‡	1.72 ± 0.43‡‡

Data are means ± SE (n = 8–10).

*Expressed in mmol/g wet wt for sciatic nerve and mmol/g protein for retina.

†Significantly different from controls ($P < 0.01$).

‡Significantly different from untreated diabetic rats ($P < 0.01$).

TABLE 3

PARP activity (mmol NAD^+ per 30 min)* in cell-free system containing PARP and NAD^+

Compound	Concentrations					
	0	10 nmol/l	100 nmol/l	1 μmol/l	10 μmol/l	100 μmol/l
300 μmol/l NAD^+						
Fidarestat	0.327 ± 0.006	0.307 ± 0.003	0.292 ± 0.017	0.312 ± 0.004	0.300 ± 0.003	0.301 ± 0.001
INO-1001	0.327 ± 0.006	0.270 ± 0.006	0.042 ± 0.0014	0.00125 ± 0.0003	0.0015 ± 0.006	0.0015 ± 0.0003
850 μmol/l NAD^+						
Fidarestat	0.315 ± 0.006	0.306 ± 0.003	0.308 ± 0.009	0.300 ± 0.006	0.309 ± 0.010	0.288 ± 0.003
INO-1001	0.315 ± 0.006	0.302 ± 0.004	0.009 ± 0.004	0.0043 ± 0.0006	0.0025 ± 0.003	0.00125 ± 0.00025

Data are means ± SE (n = 4–7).

*The potent PARP inhibitor INO-1001 was used as a positive control.